ISSN 1392–1320 MATERIALS SCIENCE (MEDŽIAGOTYRA). Vol. 11, No. 2. 2005

The Effect of Loading Direction and Pores Distribution Mode on Porous Polymer Material Stress Concentration

Daiva ZELENIAKIENĖ[1*], Tadas KLEVECKAS[2], Jonas LIUKAITIS[2]

[1]*Department of Mechanics of Solids, Kaunas University of Technology, Kęstučio 27, LT-44025 Kaunas, Lithuania*
[2]*Department of Clothing and Polymer Products Technology, Kaunas University of Technology, Studentų 56, LT-51424 Kaunas, Lithuania*

Received 14 January 2005; accepted 06 March 2005

The determination of microstructure influence on porous materials macro properties can be applied to predict behaviour of material. The numerical finite element method was used to identify stress concentration factor of porous polymer material microstructure in dependence on loading direction, porosity and pores distribution mode under tensile loading by constant strain. It was determined that the value of stress concentration factor depends upon the orientation of matrix microstrips with respect to loading direction and the stiffness changes of the matrix adjacent zones. If the high stiffness changes of the matrix adjacent zones are characteristic and the longitudinal axis of thin microstrips is in line with the direction of tensile, the stress concentration factor of porous structure is the highest. If the angle between these microstrips and the direction of tensile is equal to 45°, the stress concentration factor is the lowest. If the low stiffness changes of the matrix, adjacent zones are characteristic such porous material exhibits low stress concentration factor without reference to loading direction.

Keywords: porous polymer, porosity, pores distribution mode, stress concentration, finite element method.

INTRODUCTION

Porous structural materials with perfect microstructure were designed by nature and as it is often happening, a man made a copy of this for his products. Currently porous materials are widely used instead of monolithic these, because they are cheaper, lighter and exhibit good strength and deformability [1]. These materials, components and products of them are widely used in the automotive industry, aviation, packaging, furniture, sewing, footwear trades. They have many fields of applications, including the manufacturing of thermal insulation, building materials, devices of buoyancy, absorbers, various filters, hydrophobic membranes, artificial leathers, shoes soles and a lot of others products [1 – 6].

Porous material is heterogeneous system with complex microstructure [7]. This system is diphase composite with solid matrix and gasiform filler [8, 9]. The spectrum of porous materials is very wide. They can be made from polymers (glassy, semi-crystalline, elastomeric), metals (aluminium, nickel, copper), ceramics [1, 10 – 14]. Macromechanical properties of heterogeneous systems depend not only on the material nature but on this morphology, also [14 – 16].

To determine the macroscopic overall characteristics of heterogeneous media is an essential problem in many engineering applications [17]. From the time and cost viewpoints, performing straightforward experimental measurements on a number of material samples, for various phase properties, volume fractions and loading histories is a hardly feasible task. On the other hand, due to the usually enormous difference in length scales involved, it is impossible, for instance, to generate a finite element mesh that accurately represents the microstructure and also allows the numerical solution of the macroscopic structural component within a reasonable amount of time on today's computational systems. To overcome this problem several homogenization methods have been created to obtain a suitable constitutive model to be inserted at the macroscopic level [18 – 27]. Most of these methods are based on the concept of a representative volume element (RVE) [17]. The homogenized material properties are determined by fitting the results of the detailed modelling of the RVE (typically performed by the finite element method) on macroscopic phenomenological equations. The material configuration to be considered is assumed to be macroscopically homogeneous (continuum mechanics theory is suitable to describe the macroscopic behaviour), but microscopically heterogeneous. The physical and geometrical properties of the microstructure are identified by the RVE. It must be selected such that the local microscopic material structure can be considered as the RVE surrounded by copies of itself, without overlapping of the RVEs and without voids between the boundaries of the RVEs. The RVE should be large enough to represent the microstructure, without introducing non-existing properties and at the same time, it should be small enough to allow efficient computational modelling [17]. This issue has been discussed in a number of studies [28].

The alternative of making approaches in RVE design of assumption on global periodicity of the microstructure, suggesting the whole macroscopic specimen consists of spatially repeated unit cells or more realistic assumption on local periodicity, i. e. the microstructure can have different morphologies corresponding to different macroscopic points, while it repeats itself in a small vicinity of each individual macroscopic point is existing. On either case the choice it is some advantages and weakness, so the decision is leaded by particular solution of a problem [29, 30]. The

[*]Corresponding author. Tel.: + 370-37-300426; fax: + 370-37-324108.
E-mail address: *Daiva.Zeleniakiene@ktu.lt* (D. Zeleniakienė)

question about the difference of the results obtained by investigation of periodic or random microstructure can be raised, also. Studies showed that for small deformations of elastomeric model there is almost no difference in the responses originating from the periodic and random pores distributions [17]. For large deformations, the difference between the response of the periodic structure and the response averaged over the random RVEs does not exceed 2 % [17]. So if the porous material with elastomeric matrix is investigated the choice of periodic structure is tenable. It results in simpler modelling and investigation of various factors influence on the materials mechanical behaviour.

In the case of periodic microstructure, the loading direction can influence on the deformation behaviour and stress concentration of the material, also. So as periodic models are investigated it is purposeful to evaluate the effect of loading direction.

The aim of this investigation was to evaluate the influence of loading direction and pores distribution mode on porous polymer material stress concentration.

EXPERIMENTAL

In order to clarify the deformation behaviour of porous polymers, computational studies have been performed. A typical porous polymer contains pores, usually which are spherical and are dispersed through the matrix. Although the distribution of the pores is somewhat random, here, it is assumed that it is periodic.

The finite element method (FEM) was used to identify influence of material porosity, pores distribution mode and tension direction on the stress concentration. Analysis was performed by finite element code ALGOR. The plane 2D model was made to utilize symmetry and periodicity, assuming that there are no trough-the thickness stresses in the plane. The exact number of elements of each model depends on model type and porosity.

To obtain the influence of loading direction and pores distribution mode, three types of plane models, which differ from each other in porous size and its distribution mode, were investigated. The obtained models are over-simplified representation of porous materials structure, which was observed in many natural or artificial composite materials. Model I was designed with one-sized pores, which lay in parallel rows with equal distance between porous in each direction. The diameter of these pores was d_1. Model II was created on the basis of Model I: symmetrically additional porous elements, diameter of which was $d_2 < d_1$, were added in interpores zones, located between pores d_1. Model III consisted pores of three sizes that varied according selected criteria: $d_3 < d_2 < d_1$. The ratio between pores diameter and main measure of RVE L (L =50 mm) was proportionally changed according to these expressions: $d_1 / L = 0.01 \div 0.20$, $d_2 / L = 0.02 \div 0.12$, $d_3 / L = 0.02 \div 0.04$. In all cases the distance between pores centers was constant. The enlarged description of theses models was presented in previous investigations [31, 32].

Fig. 1 illustrates the computational model in which pores are assumed to be distributed periodically. There it is presented the case of the Model III, but the scheme is analogous for all investigated models. The boundary conditions on the macroscopic scale are that the upper surface is shear-free with a constant displacement constraint; the bottom surface has constraint on two directions in the point in the symmetry axe of model and this on one direction in other points as shown in Fig. 1. Whereas the right and left surfaces are assumed to be stress free. The total relative strain is 0.2.

In order to investigate the effect of loading direction on the deformation behaviour the angle θ, which is the angle of the tension direction with respect to the principal direction of the unit cell, is introduced and is parametrically varied from 0° to 45°.

Young's modulus of matrix material is E = 3.98 MPa and Poison's rate is μ = 0.46. This material was used for previous investigations, so the choice of this material is done for comparison purposes.

RESULTS AND DISCUSSIONS

Model I. The angle of loading direction is the angle of microstrips orientation in the Model I. The relationship of maximal stress concentration factor K_σ of this model with respect to the angle θ of loading direction and porosity γ_p is presented in the Fig. 2. It seems that, the increase of porosity up to the value equal to 0.5 the stress concentration factor decreases. In all investigated porosity range the stress concentration factor is the highest when θ = 0°. In this case, the longitudinal axis of microstrips superposes with the direction of tensile. As the θ increases the stress factor decreases and it is the lowest when θ = 45°. It could be explained using the RVE of Model I made from four unit cells (Fig. 3). In the cases of θ = 0°

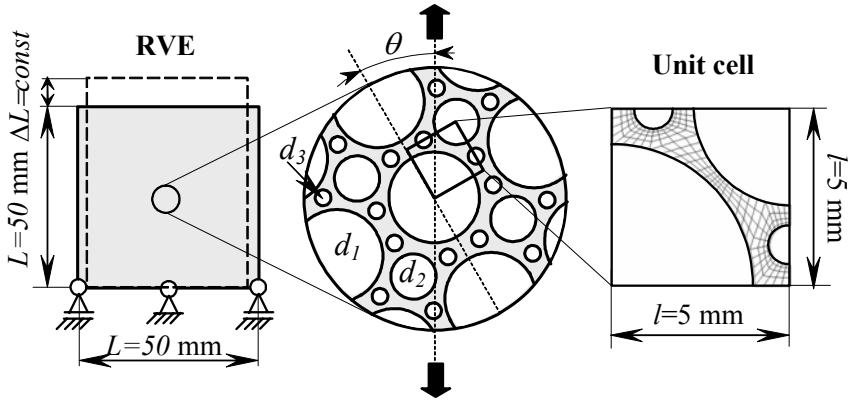

Fig. 1. Computational model. Heterogeneous pores of RVE are assumed to be circular cylinders of diameter d_1, d_2 and d_3 contained in the unit cell, which is the microscopic element of the porous material

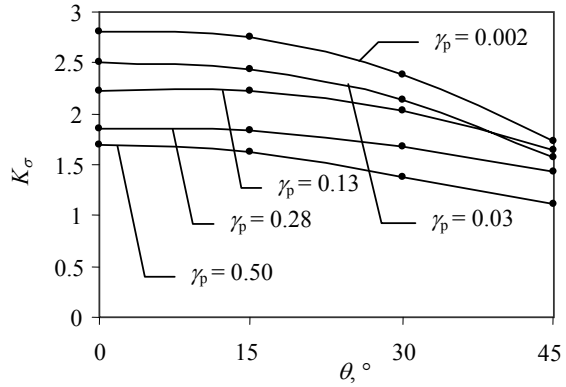

Fig. 2. The relationship of maximal stress concentration factors K_σ with respect to the angle θ of loading direction and porosity γ_p for Model I

and $\theta = 45°$, it can be written maximal and minimal lengths of RVE cross-section in all of these cases:

$$a_{\max 0°} = 2l, \tag{1}$$

$$a_{\min 0°} = 2l - 2\frac{d_1}{2} = 2l - d_1, \tag{2}$$

$$a_{\max 45°} = \sqrt{\left(2l - \frac{d_1}{2}\right)^2 + \left(2l - \frac{d_1}{2}\right)^2} = \sqrt{2\left(2l - \frac{d_1}{2}\right)^2} = \\ = \sqrt{2}\left(2l - \frac{d_1}{2}\right) = 2\sqrt{2}l - \frac{\sqrt{2}}{2}d_1 = \\ = 2.83l - 0.705d_1, \tag{3}$$

$$a_{\min 45°} = \sqrt{(2l)^2 + (2l)^2} - 2\frac{d_1}{2} = \sqrt{8l^2} - d_1 = \\ = 2.83l - d_1, \tag{4}$$

where $a_{\max 0°}$ and $a_{\max 45°}$ are the maximal lengths of RVE cross-section respectively as $\theta = 0°$ and $\theta = 45°$, $a_{\min 0°}$ and $a_{\min 45°}$ are the minimal lengths of RVE cross-section respectively as $\theta = 0°$ and $\theta = 45°$ (Fig.3). The differences of RVE cross-section lengths are obtained by subtraction of the maximal and minimal lengths:

$$\left(a_{\max 0°} - a_{\min 0°}\right)H = \left(2l - 2l + d_1\right)H = d_1 H, \tag{5}$$

$$\left(a_{\max 45°} - a_{\min 45°}\right)H = \left(2.83l - 0.705d_1 - 2.83l + d_1\right)H = \\ = 0.295d_1 H. \tag{6}$$

So, from (5) and (6) it is clear seen that the difference of RVE cross-section lengths as $\theta = 0°$ is about 3 times higher than this as $\theta = 45°$. In the Fig. 3 seems that the differences of RVE cross-section lengths as $\theta = 15°$ and $\theta = 30°$ are mediate.

As the difference of tensile stiffness depends on the difference of RVE cross-section, it is clear that the highest difference of tensile stiffness of Model I is as angle of loading direction is equal to zero and the lowest difference of this is as $\theta = 45°$. Therefore if the longitudinal axis of thin microstrips is in line with the direction of tensile, the stress concentration factor is the highest. If the angle between microstrips and the direction of tensile is equal to 45°, the stress concentration factor is the lowest.

The distribution of stress concentration factor K_σ near pores d_1 for Model I as the angle of loading direction is varying from 0° to 45° and $\gamma_p = 0.002$ is shown in Fig. 4. It seems that, the maximum of stress concentration factor is decreasing and the location of this maximum is moving by angle θ as this angle increases from 0° to 45°

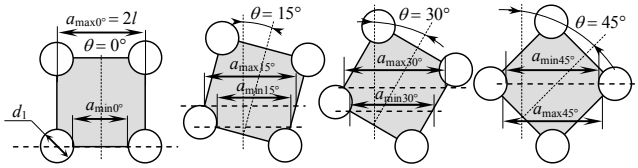

Fig. 3. The RVE of Model I made from four unit cells as the angle θ of loading direction is varying

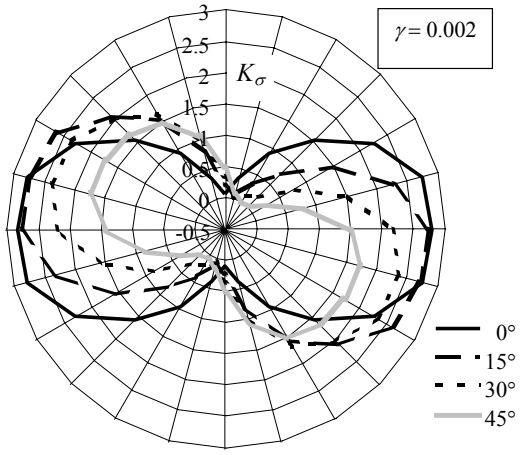

Fig. 4. The stress concentration factor K_σ near pores d_1 for Model I as the angle of loading direction is varying

Model II. The influence of angle θ of loading direction and porosity γ_p on the maximal stress concentration factor changes for Model II is presented in Fig. 5. The porosity value results in the dependence mode.

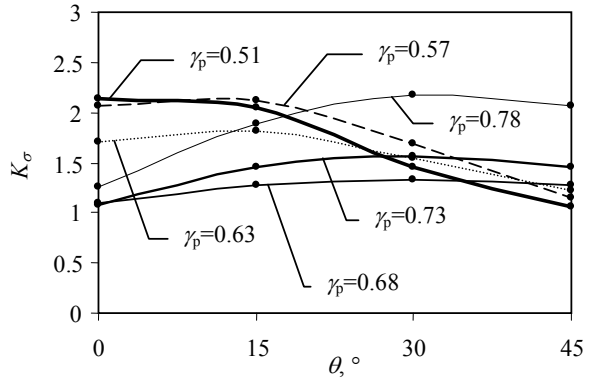

Fig. 5. The relationship of maximal stress concentration factors K_σ with respect to the angle θ of loading direction and porosity γ_p for Model II

Decreasing dependences are characteristic for low porosity value models. Increasing dependences are characteristic for high porosity value models. Two kinds of microstrips are in the Model II. Ones of them are the same like in the Model I formed between pores d_1 and the angle of loading direction is equal to the angle of these microstrips orientation. Others of them formed between pores d_1 and d_2 and the angle between their longitudinal axis and tension direction is equal to 45°. So, the stress

concentration factor of Model II depends on both the microstrips orientation with respect to the load direction and the thickness of microstrips. In the case of lower porosity ($\gamma_p = 0.51 \div 0.63$) Model II exhibits very small pores d_2. The thinner microstrips are formed between pores d_1 the bigger influence of them on stress concentration factor is. Therefore, the dependence of stress concentration factor upon the angle of loading direction has the same character like in the case of Model I. In the case of higher porosity ($\gamma_p = 0.68 \div 0.79$) the thinner microstrips are formed between pores d_1 and d_2 the higher influence of them on stress concentration factor is. As the angle θ increases thin strips are oriented in the direction of tension and the stress concentration factor increases.

The stress concentration factor K_σ near pores d_1 for Model II as the angle of loading direction is varying and porosity is equal to 0.51 is presented in Fig. 6. As the angle of loading direction increases, the stress concentration factor near pore d_1 decreases as in the case of Model I. Therefore, the decrease of Model II stress concentration factor near d_1 as $\gamma_p = 0.51$ is leaded by decreasing of microstrips between pores d_1 stiffness differences as θ is increasing.

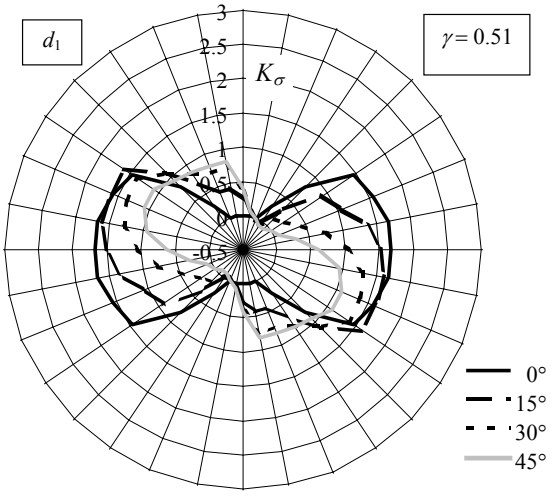

Fig. 6. The stress concentration factor K_σ near pores d_1 for Model II as the angle of loading direction is varying

When porosity is low and $\theta = 0°$ the stress concentration factor near pores d_2 is high (Fig. 7). As it was determined before [31] in the case of low porosity of Model II, small pores d_2 act as stress concentrators. Besides, pores d_2 fall into the zone of high shear stress as $\theta = 0°$ [33]. It decides the high stress concentration factor near pores d_2. The increasing of loading direction angle results in the decrease of stress concentration factor. That is the reason of shear stress decreasing as the pores d_2 pass into the other position. So, as $\theta = 45°$ K_σ near d_2 is lower than this near pore d_1.

The changes of stress concentration factor of Model II near pores d_1 and d_2 when the angle of loading direction is varying and porosity value is high are presented in Fig. 8 and Fig. 9. It seems that four maximums of stress concentration factor near both pores d_1 and d_2 are formed in the zones of thin microstrips between pores d_1 and d_2 without reference to loading direction. The increasing of θ does not results in changes of stress concentration factor because in this high porosity case microstrips between pores d_1 and d_2 are very thin and in all investigates loading direction cases are like stress concentrators.

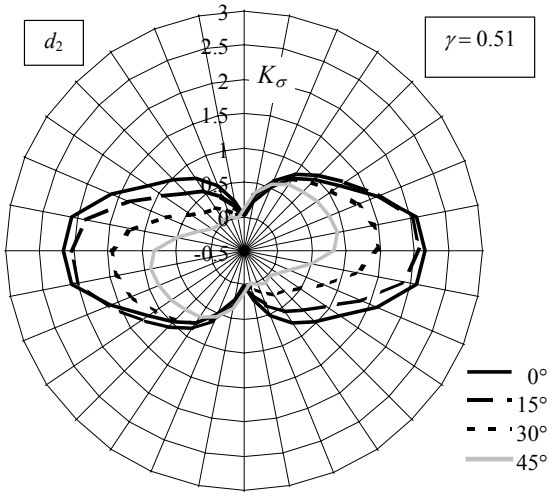

Fig. 7. The stress concentration factor K_σ near pores d_2 for Model II as the angle of loading direction is varying

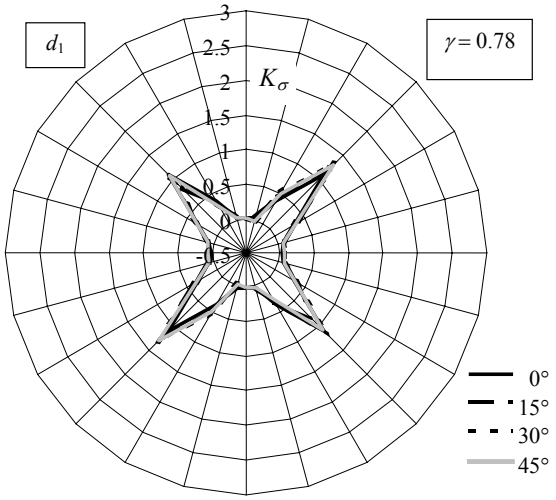

Fig. 8. The stress concentration factor K_σ near pores d_1 for Model II as the angle of loading direction is varying

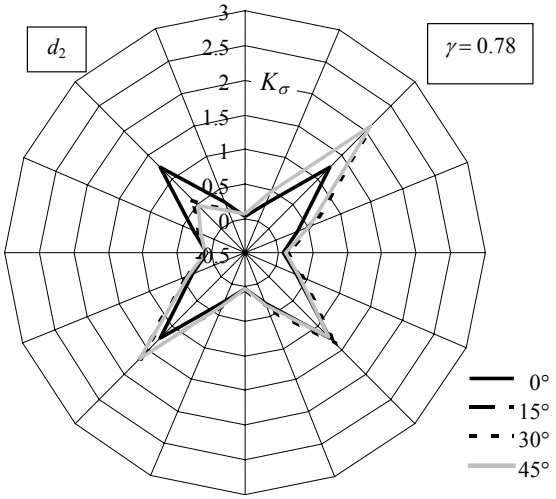

Fig. 9. The stress concentration factor K_σ near pores d_2 for Model II as the angle of loading direction is varying

Model III. The influence of angle θ of loading direction and porosity γ_p on the maximal stress concentration factor changes for Model III is presented in Fig. 10. It seems that as $\gamma_p = 0.76$ the highest stress concentration factor is when $\theta = 30°$ and as $\gamma_p = 0.87$ it is as $\theta = 15°$. However, the influence of loading direction on stress concentration factor of Model III is low comparing to Model I and Model II. If in the case of Model II the maximal difference of stress concentration factor values is 50 % that in the case of Model III this difference is 16 %. The insignificant influence of loading direction is seen in Fig. 11 -13 where the stress concentration factor K_σ near pores d_1, d_2 and d_3 for Model III as the angle of loading direction varies is presented. This is leaded by low stiffness changes of the matrix adjacent zones in all directions.

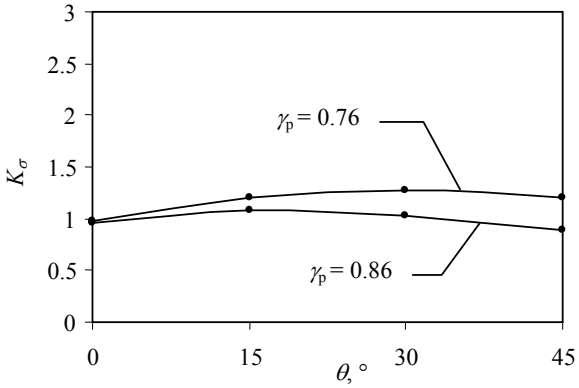

Fig. 10. The relationship of maximal stress concentration factors K_σ with respect to the angle θ of loading direction and porosity γ_p for Model III

So the obtained results certified the decrease of stress concentration factor due to the decrease of stiffness changes of the matrix adjacent zones what was determined before [31, 32]. In all investigated loading direction angles cases the inequality is valid

$$K_{\sigma\max \text{ of Model I}} > K_{\sigma\max \text{ of Model II}} > K_{\sigma\max. \text{ of Model III}}. \quad (7)$$

That means the stress concentration factor of Model III is the lowest in which the lowest stiffness changes of the matrix adjacent zones are characteristic. The stress concentration factor of Model I is the highest in which the highest stiffness changes are characteristic.

CONCLUSIONS

It was determined that the stress concentration factor of porous periodic polymer material structure depends upon the orientation of matrix microstrips with respect to loading direction and on the stiffness changes of the matrix adjacent zones as the loading is the constant strain ($\varepsilon = 0.2$).

If the high stiffness changes of the matrix adjacent zones are characteristic and the longitudinal axis of thin microstrips is in line with the direction of tensile, the stress concentration factor of porous structure is the highest. If the angle between these microstrips and the tensile direction is equal to 45°, the stress concentration factor is the lowest.

If the low stiffness changes of the matrix, adjacent zones are characteristic such porous material exhibits low stress concentration factor without reference to loading direction.

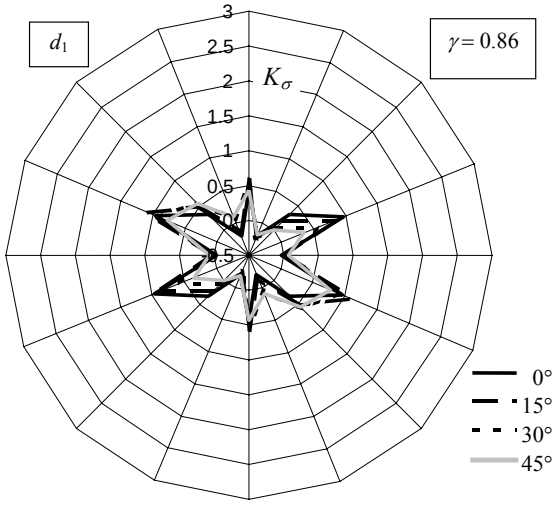

Fig. 11. The stress concentration factor K_σ near pores d_1 for Model III as the angle of loading direction is varying

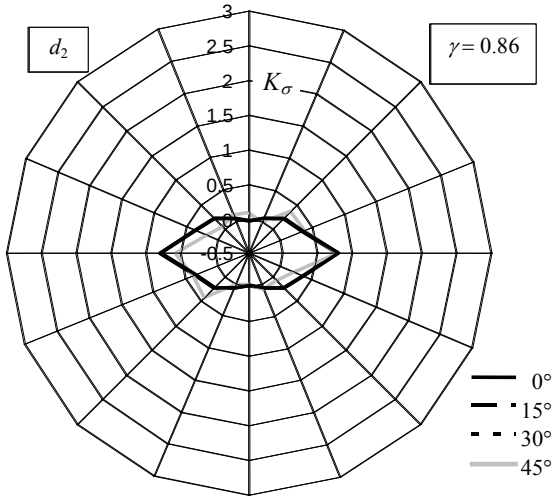

Fig. 12. The stress concentration factor K_σ near pores d_2 for Model III as the angle of loading direction is varying

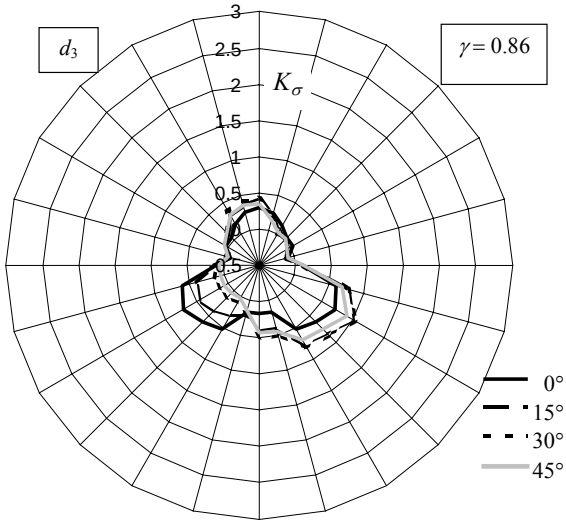

Fig. 13. The stress concentration factor K_σ near pores d_3 for Model III as the angle of loading direction is varying

REFERENCES

1. **Gibson, L. J.; Ashby, M. F.** Cellular Solids: Structure and Properties. Cambridge, Cambridge University Press, 1997: 510 p.
2. **Everett, R. K., Matic, P., Harvey II, D. P., Kee, A.** The Microstructure and Mechanical Response of Porous Polymers *Materials Science and Engineering A* 249 1998: pp. 7 – 13.
3. **Park, C., Nutt, S. R.** Strain Rate Sensitivity and Defects in Steel Foam *Materials Science and Engineering A* 232 2002: pp. 358 – 366.
4. **Thomas, T., Muhfuz, H., Carlsson, L. A., Kanny, K., Jeelani, S.** Dynamic Compression of Cellular Cores: Temperature and Strain Rate Effects *Composite Structures* 58 (4) 2002: pp. 505 – 512.
5. **Mills, N. J.** Micromechanics of Polymeric Foams *Proceedings of 3rd Nordic Meeting on Materials and Mechanics, Aalborg, Denmark* 2000: pp. 45 – 76.
6. **Andrews, E. W., Gibson, L. J.** The Influence of Cracks-Like Defects on the Tensile Strength of an Open-Cell Aluminum Foam *Scripta Materialia* 44 2001: pp. 1005 – 1010.
7. **Roberts, A. P., Knackstedt, M. A.** Structure - Property Correlations in Model Composite Materials *Physical Review E* 54 1996: pp. 2313 – 2328.
8. **Kalamkarov, A. L., Kolpakov, A. G.** Analysis, Design and Optimization of Composite structures. Chichester, John Wiley & Sons, 1997: 356 p.
9. **Mills, N. J., Fitzgerald, C., Gilchrist, A., Verdejo, R.** Polymer Foams for Personal Protection: Cushions, Shoes and Helmets *Composites Science and Technology* 63 (16) 2003: pp. 2389 – 2400.
10. **Kakavas P. A., Anifantis N. K.** Effective Moduli of Hyperelastic Porous Media at Large Deformation *Acta Mechanica* 160 2003: pp. 127 – 147.
11. **Kanny, K., Muhfuz, H., Carlsson, L. A., Thomas, T., Jeelani, S.** Dynamic Mechanical Analyses and Flexural Fatigue of PVC Foams *Composite Structures* 58 (2) 2002: pp. 175 – 183.
12. **Andrews, E. W., Huang, J.- S., Gibson, L. J.** Creep Behavior of a Closed - Cell Aluminum Foam *Acta Materialia* 47 (10) 1999: pp. 2927 – 2935.
13. **Ruan, D., Lu, G., Chen, F. L., Siores, E.** Compressive Behaviour of Aluminum Foams at Low and Medium Strain Rates *Composite Structures* 57 2002: pp. 331 – 336.
14. **Roberts, A. P., Garboczi, E. J.** Elastic Properties of Model Porous Ceramics *Journal of the American Ceramic Society* 83 (12) 2000: pp. 3041 – 3058.
15. **Schlei, B. R., Prasad, L., Skourikhine, A. N.** Geometric Morphology of Cellular Solids *Proceedings of SPIE* 4476 2001: pp. 73 – 79.
16. **Roberts, A. P., Garboczi, E. J.** Elastic Moduli of Model Random Three - Dimensional Closed – Cell Cellular Solids *Acta Materialia* 49 (2) 2001: pp. 189 – 197.
17. **Kouznetsova, V., Brekelmans, W. A. M., Baaijens, F. P.** An Approach to Micro - Macro Modeling of Heterogeneous Materials *Computational Mechanics* 27 (1) 2001: pp. 37 – 48.
18. **Theocaris, P. S., Stavroulakis, G. E.** The Homogenization Method for the Study of Variation of Poisson's Ratio in Fiber Composites *Applied Mechanics* 68 1998: pp. 281 – 295.
19. **Nishiwaki, S., Frecker, M. I., Min, S., Kikuchi, N.** Topology Optimization of Compliant Mechanisms Using the Homogenization Method *International Journal for Numerical Methods in Engineering* 42 1998: pp. 535 – 559.
20. **Fish, J., Yu, Q., Shek, K.** Computational Damage Mechanics for Composite Materials Based on Mathematical Homogenization *International Journal for Numerical Methods in Engineering* 45 1999: pp. 1657 – 1679.
21. **Moës, N., Oden, J. T., Vemaganti, K. Remacle, J. F.** Simplified Methods and a Posteriori Error Estimation for the Homogenization of Representative Volume Elements (RVE) *Computer Methods in Applied Mechanics and Engineering* 176 1999: pp. 265 – 278.
22. **Cabrillac, R. Malou, Z.** Mechanical Modelization of Anisotropic Porous Materials with a Homogenization Method. Application to Aerated Concretes *Construction and Building Materials* 14 2000: pp. 25 – 33.
23. **Takano, N., Ohnishi, Y., Zako, M. Nishiyabu, K.** The Formulation of Homogenization Method Applied to Large Deformation Problem for Composite Materials *International Journal of Solids and Structures* 37 2000: pp. 6517 – 6535.
24. **Sun, H., Di, S., Zhang, N., Wu, C.** Micromechanics of Composite Materials Using Multivariable Finite Element Method and Homogenization Theory *International Journal of Solids and Structures* 38 2001: pp. 3007 – 3020.
25. **Okada, H., Fukui, Y., Kumazawa, N.** Homogenization Method for Heterogeneous Material Based on Boundary Element Method *Computers & Structures* 79 2001: pp. 1987 – 2007.
26. **Miehe, C., Schröder, J., Becker, M.** Computational Homogenization Analysis in Finite Elasticity: Material and Structural Instabilities on the Micro- and Macro - Scales of Periodic Composites and Their Interaction *Computer Methods in Applied Mechanics and Engineering* 191 2002: pp. 4971 – 5005.
27. **Matsui, K., Terada, K., Yuge, K.** Two - Scale Finite Element Analysis of Heterogeneous Solids with Periodic Microstructures *Computers & Structures* 82 2004: pp. 593 – 606.
28. **Terada, T., Hori, M., Kyoya, T., Kikuchi, N.** Simulation of the Multi - Scale Convergence in Computational Homogenization Approch *International Journal of Solids and Structures* 37 2000: pp. 2285 – 2311.
29. **Smit, R. J. M., Brekelmans, W. A. M., Meijer, H. E. H.** Prediction of the Mechanical Behavior of Nonlinear Heterogeneous Systems by Multi - Level Finite Element Modeling *Computer Methods in Applied Mechanics and Engineering* 155 1998: pp. 181 – 192.
30. **Lahellec, N., Mazerolle, F., Michel. J. C.** Second - Order Estimate of the Macroscopic Behavior of Periodic Hyperelastic Composites: Theory and Experimental Validation *Journal of the Mechanics and Physics of Solids* 52 2004: pp. 27 – 49.
31. **Zeleniakiene, D., Kleveckas, T., Liukaitis, J., Fataraite, E.** The Influence of Porosity Value and Mode on Soft Materials Behaviour *Materials Science* (*Medžiagotyra*) 9 2003: pp. 201 – 205.
32. **Zeleniakiene, D., Kleveckas, T., Liukaitis, J., Marazas, G.** The Influence of Porosity on Stress and Strain State of Porous Polymer Materials *Materials Science* (*Medžiagotyra*) 9 2003: pp. 358 – 362.
33. **Tomita, Y., Lu, W.** Characterization of Micro- to Macroscopic Response of Polymers Containing Voids under Macroscopically Uniform Deformation *International Journal of Solids and Structures* 39 2002: pp. 3409 – 3428.

DOI: 10.5755/j02.ms.26499